© 2014. Published by The Company of Biologists Ltd | Journal of Cell Science (2014) 127, 295–304 doi:10.1242/jcs.127357

RESEARCH ARTICLE

The tumor suppressor Lgl1 forms discrete complexes with NMII-A and Par6α–aPKCζ that are affected by Lgl1 phosphorylation

Inbal Dahan, Daria Petrov, Einav Cohen-Kfir and Shoshana Ravid*

ABSTRACT

Non-muscle myosin IIA (NMII-A) and the tumor suppressor lethal giant larvae 1 (Lgl1) play a central role in the polarization of migrating cells. Mammalian Lgl1 interacts directly with NMII-A, inhibiting its ability to assemble into filaments *in vitro*. Lgl1 also regulates the cellular localization of NMII-A, the maturation of focal adhesions and cell migration. In *Drosophila*, phosphorylation of Lgl affects its association with the cytoskeleton. Here we show that phosphorylation of mammalian Lgl1 by aPKCζ prevents its interaction with NMII-A both *in vitro* and *in vivo*, and affects its inhibition of NMII-A filament assembly. Phosphorylation of Lgl1 affects its cellular localization and is important for the cellular organization of the acto-NMII cytoskeleton. We further show that Lgl1 forms two distinct complexes *in vivo*, Lgl1–NMIIA and Lgl1–Par6α–aPKCζ, and that the formation of these complexes is affected by the phosphorylation state of Lgl1. The complex Lgl1–Par6α–aPKCζ resides in the leading edge of the cell. Finally, we show that aPKCζ and NMII-A compete to bind directly to Lgl1 at the same domain. These results provide new insights into the mechanism regulating the interaction between Lgl1, NMII-A, Par6α and aPKCζ in polarized migrating cells.

KEY WORDS: Cell motility, Lethal giant larvae (Lgl), Non-muscle myosin

INTRODUCTION

Cell migration is a highly integrated multistep process involving coordinated cytoskeletal remodeling (Lauffenburger and Horwitz, 1996; Mitchison and Cramer, 1996). The basic steps involved are: polarizaton of the cell; extention of an actin-rich protrusion from the leading edge; establishment of new adhesion sites in the new protrusion; pulling the cell body forward in the direction of the new attachment sites; and, finally, detachment of the rear of the cell and tail retraction (Lauffenburger and Horwitz, 1996; Mitchison and Cramer, 1996; Ridley et al., 2003). Non-muscle myosin II (NMII), an actin-based motor protein, plays a key role in cell migration through its effects on cell polarity, adhesion, lamellar protrusion and rear retraction (Conti and Adelstein, 2008; Jay et al., 1995; Verkhovsky et al., 1999; Vicente-Manzanares et al., 2009).

NMII is a hexamer composed of two heavy chains of ~200 kDa and two pairs of essential and regulatory light chains (Vicente-Manzanares et al., 2009). The NMII heavy chains consist of an N-terminal globular head domain and a tail domain. The tail domain includes an α-helical coiled-coil-forming rod and a non-helical tailpiece on the C-terminus. The α-helical coiled-coil domain is responsible for assembly of NMII monomers into filaments, which are the functional structures required for NMII activity (Dulyaninova et al., 2005; Even-Faitelson and Ravid, 2006; Murakami et al., 2000; Ronen and Ravid, 2009; Rosenberg and Ravid, 2006). Vertebrates have three different NMII isoforms, NMII-A, NMII-B and NMII-C that differ in their heavy chain sequences, in the kinetics of their ATPase activity, in their subcellular localization and in their functions in cell polarization during migration (Golomb et al., 2004; Katsuragawa et al., 1989; Kolega, 1998; Shohet et al., 1989; Simons et al., 1991; Vicente-Manzanares et al., 2009). In migrating cells NMII-A is dynamic and assembles actomyosin bundles in protrusions (Cai et al., 2006; Vicente-Manzanares et al., 2007), whereas NMII-B incorporates into preformed actin bundles, remains stationary, and defines the center and rear of the migrating cell (Vicente-Manzanares et al., 2008).

Recently we showed that NMII-A and the mammalian homolog of the tumor suppressor Lethal (2) giant larvae (Lgl; also known as L(2)gl) play a central role in the polarization of migrating cells (Dahan et al., 2012). Lgl is a tumor suppressor protein essential for the development of polarized epithelia, for cell polarity associated with asymmetric cell division of neuroblasts during fly development and for the correct polarization of migrating cells (Bilder et al., 2000; Bilder and Perrimon, 2000; Dahan et al., 2012; Ohshiro et al., 2000; Peng et al., 2000). Lgl is composed of two domains, the N-terminal region folds into two β-propellers. These provide docking platforms for simultaneous interactions with a number of proteins. The C-terminal domain is an Lgl-family-specific domain containing several conserved serine residues which are targeted for phosphorylation by atypical protein kinase C isoform ζ (aPKCζ) (Betschinger et al., 2003; Plant et al., 2003; Vasioukhin, 2006).

Mammalian cells express two Lgl homologs, Lgl1 and Lgl2 (also known as Llgl and Llgl2). Lgl1 is expressed almost ubiquitously, whereas Lgl2 is expressed in a tissue-specific manner (Klezovitch et al., 2004; Sripathy et al., 2011). In cultured cell lines and in mouse brain, Par6, aPKC and Lgl form a multiprotein polarity complex in which Lgl is targeted for phosphorylation by aPKCζ (Betschinger et al., 2003; Plant et al., 2003). This phosphorylation is important for the correct polarization of embryonic fibroblasts in response to wounding (Plant et al., 2003) and for centrosome reorientation in astrocytes (Etienne-Manneville, 2008).

Biochemical and genetic analyses suggest that the *Drosophila* Lgl is a component of the cytoskeleton that interacts with NMII and that this interaction is regulated by the phosphorylation of Lgl

Department of Biochemistry and Molecular Biology, The Institute of Medical Research Israel-Canada, The Hebrew University – Hadassah Medical School, Jerusalem 91120, Israel.

*Author for correspondence (shoshr@ekmd.huji.ac.il)

Received 16 January 2013; Accepted 15 October 2013

Journal of Cell Science

Journal of Cell Science (2014) 127, 295–304 doi:10.1242/jcs.127357

(Betschinger et al., 2005; Kalmes et al., 1996; Strand et al., 1994). Recently we showed that in mammalian cells Lgl1 interacts directly with NMII-A through a domain containing the phosphorylation sites for aPKCζ (Dahan et al., 2012). Lgl1 interaction with NMII-A inhibits NMII-A filament assembly *in vitro*, excludes NMII-A from the leading edge of the cell and regulates the morphology of focal adhesions (Dahan et al., 2012). We proposed that the interaction between Lgl1 and NMII-A is electrostatic and that phosphorylation of Lgl1 decreases the positive charge of the interacting domain of Lgl1, thus preventing it from binding to NMII-A (Dahan et al., 2012). This hypothesis fits previous findings that phosphorylation of *Drosophila* Lgl dissociates it from the cytoskeleton (Betschinger et al., 2005). The experiments reported here reveal that phosphorylation of Lgl1 by aPKCζ affects its interaction with NMII-A both *in vitro* and *in vivo*. We show that Lgl1 forms two distinct complexes, Lgl1–NMIIA and Lgl1–Par6α–aPKCζ and that NMII-A and aPKCζ compete for binding to Lgl1. Furthermore, we demonstrate that Lgl1 phosphorylation affects its cellular localization and the organization of the acto-NMII cytoskeleton.

RESULTS

Phosphorylation of Lgl1 affects its interaction with NMII-A

Studies in *Drosophila* indicate that Lgl is associated with NMII (Strand et al., 1994), and that phosphorylation of *Drosophila* Lgl possibly dissociates it from the cytoskeleton (Betschinger et al., 2005). In human Lgl2, serine residues 649, 653 and 660 are important for its phosphorylation *in vitro*, and serine 653 in human Lgl2 and the corresponding serine residue 659 in human Lgl1 are phosphorylated *in vivo* (Yamanaka et al., 2003). We recently showed that mammalian Lgl1 interacts directly with NMII-A, inhibiting its ability to assemble into filament *in vitro* (Dahan et al., 2012). To investigate whether phosphorylation of Lgl1 by aPKCζ affects its interaction with NMII-A, we created phosphomimetic, as well as unphosphorylatable, mouse Lgl1 C-terminal fragments involving serine residues 658, 662 and 669, corresponding to serines 649, 653 and 660 in the human Lgl1. These phospho-mutant Lgl1 C-terminal fragments were fused to maltose binding protein, MBP–Lgl1-C^{Asp} and MBP–Lgl1-C^{Ala}, respectively (Fig. 1A). These Lgl1 C-terminal phospho-mutant protein fragments were incubated with a NMII-A C-terminal fragment (NMII-A Rod, Fig. 1B) and subjected to a pull-down assay. MBP–Lgl1-$C^{\Delta MBD}$ (Fig. 1A), which lacks the NMII-A-binding site (Dahan et al., 2012), was used as a negative control. MBP–Lgl1-C^{WT} and MBP–Lgl1-C^{Ala} clearly co-precipitated with NMII-A Rod (Fig. 2A). In contrast, MBP–Lgl1-C^{Asp}, like MBP–Lgl1-$C^{\Delta MBD}$, did not co-precipitate with NMII-A Rod (Fig. 2A). These results indicate that Lgl1 phosphorylation by aPKCζ plays an important role in the interaction between Lgl1 and NMII-A Rod *in vitro*.

To test the effect of Lgl1 phosphorylation on its interaction with NMII-A *in vivo*, we examined the ability of Lgl1 C-terminal phospho-mutant protein fragments to bind to endogenous NMII-A in a cell extract obtained from the NIH 3T3 cell line (Fig. 2B). Similar to the *in vitro* results, only traces of endogenous NMII-A co-precipitated with MBP–Lgl1-C^{Asp}, whereas much more co-precipitated with MBP–Lgl1-C^{WT} and MBP–Lgl1-C^{Ala} (Fig. 2B).

To further study the effect of Lgl1 phosphorylation on its interaction with NMII-A *in vivo*, we transfected HEK293T cells with full-length Lgl1 tagged with GFP (GFP–$Lgl1^{WT}$, GFP–$Lgl1^{Asp}$ and GFP–$Lgl1^{Ala}$) and performed a co-immunoprecipitation assay using endogenous NMII-A. GFP–$Lgl1^{WT}$ and GFP–$Lgl1^{Ala}$ but not GFP–$Lgl1^{Asp}$

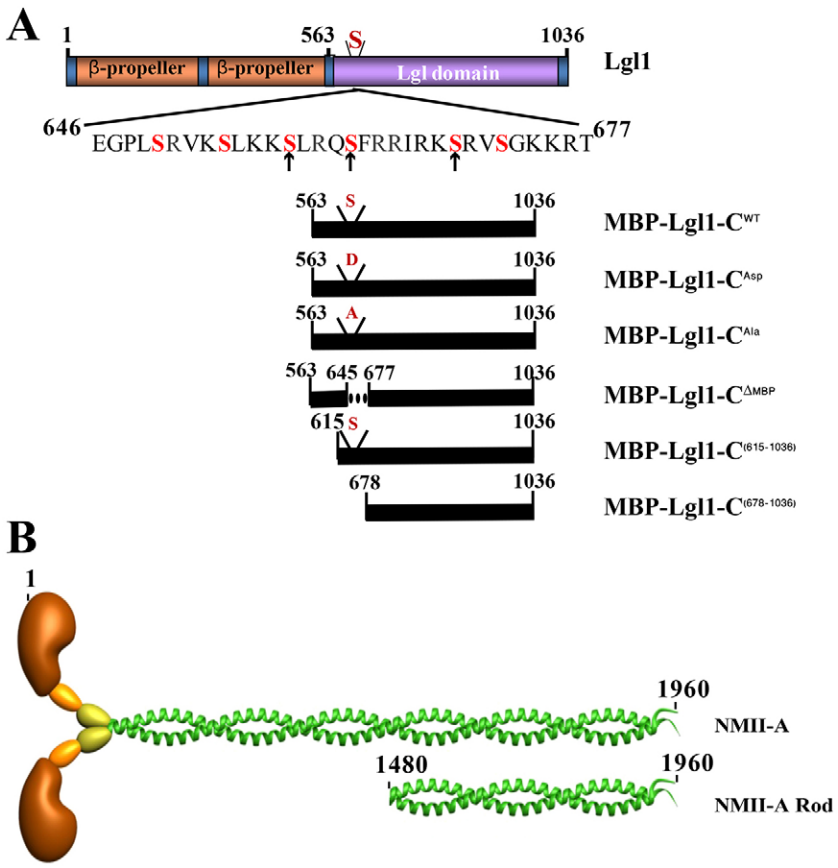

Fig. 1. Schematic representation of protein fragments used in this study. (A) Lgl1 and (B) NMII-A. Serine targets (S) for aPKCζ are indicated with arrows. These serines in positions 658, 662 and 669 in the mouse full-length Lgl1 that were converted to aspartate or alanine residues are labeled D and A, respectively. MBP–Lgl1-$C^{\Delta MBD}$ is a C-terminal fragment with an internal deletion of amino acid residues 645–677, which lacks the NMII-A-binding site (Dahan et al., 2012). Numbers indicate amino acid positions in the full-length proteins.

Journal of Cell Science (2014) 127, 295–304 doi:10.1242/jcs.127357

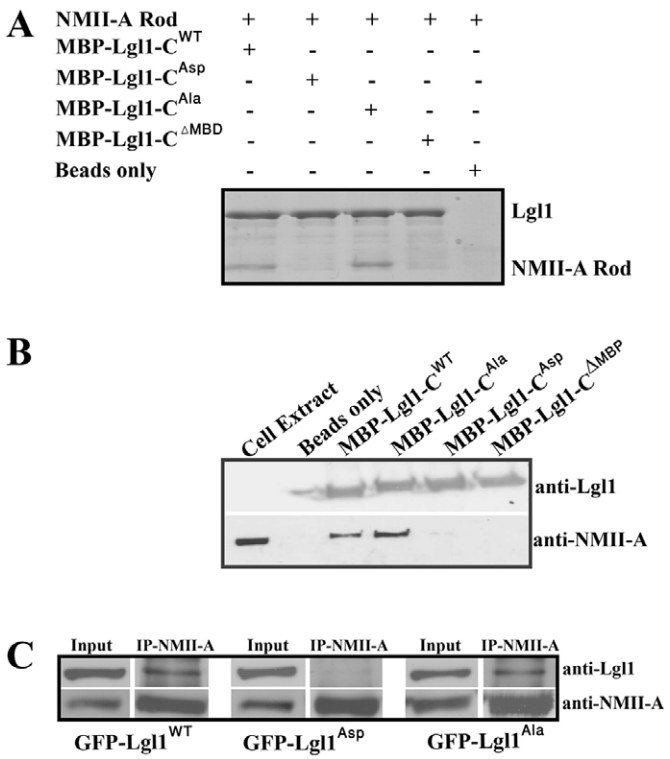

Fig. 2. Phosphorylation of Lgl1 affects the NMII-A–Lgl1 interaction. (A) Lgl1 C-terminal phospho-mutant protein fragments fused to MBP were incubated with NMII-A Rod and subjected to a pull-down assay. The proteins were detected by SDS-PAGE. MBP–Lgl1-C$^{\Delta MBD}$ and maltose beads served as negative controls. (B) Lgl1 C-terminal phospho-mutant protein fragments were incubated with NIH 3T3 cell lysate and subjected to a pull-down assay. The proteins were detected by immunoblotting with antibodies against NMII-A and Lgl1. MBP–Lgl1-C$^{\Delta MBD}$ was used as a negative control. (C) HEK293T cells were transfected with GFP–Lgl1 phospho-mutants and subjected to immunoprecipitation using NMII-A-specific antibody. The immunoprecipitated proteins were analyzed by immunoblotting with antibodies against NMII-A and Lgl1.

co-immunoprecipitated with NMII-A (Fig. 2C). These results indicate that phosphorylation of Lgl1 prevents its interaction with NMII-A both *in vitro* and *in vivo*.

Because Lgl1 binding to NMII-A Rod inhibits its ability to assemble into filaments (Dahan et al., 2012), we examined the effect of MBP–Lgl1-C phospho-mutants on NMII-A Rod filament assembly. To do this we induced NMII-A Rod filament assembly in the presence of MBP–Lgl1-C^{WT}, MBP–Lgl1-C^{Asp} MBP–Lgl1-C^{Ala} and MBP–Lgl1-C$^{\Delta MBD}$. Without the addition of Lgl1, 73% of NMII-A Rod assembled into filaments. However, in the presence of MBP–Lgl1-C^{WT} or MBP–Lgl1-C^{Ala}, NMII-A Rod filament assembly decreased to 48% and 38%, respectively (supplementary material Fig. S1). Addition of MBP–Lgl1-C^{Asp} or MBP–Lgl1-C$^{\Delta MBD}$ had only a minor effect, with 69% and 70% of NMII-A Rods assembled into filaments, respectively (supplementary material Fig. S1). Thus, the phosphorylation state of Lgl1 affects the degree of NMII-A filament inhibition.

Phosphorylation of Lgl1 is important for its proper cellular localization

We recently demonstrated that Lgl1 regulates the polarity of migrating cells by its cellular localization and by controlling the assembly state of NMII-A (Dahan et al., 2012). Because Lgl1 phosphorylation regulates its interaction with NMII-A as well as its inhibitory effect on NMII-A (Fig. 2 and supplementary material Fig. S1), we tested the effect of Lgl1 phosphorylation on its cellular localization. aPKCζ$^{-/-}$ primary embryo fibroblasts (Leitges et al., 2001) and control cells were transfected with GFP-Lgl1^{WT}. Control cells were also transfected with GFP-Lgl1^{Ala} or GFP-Lgl1^{Asp}. These cells were subjected to a scratch wound assay to produce polarized migrating cells, and the cellular localization of the GFP-tagged proteins was determined (Fig. 3A,B and supplementary material Fig. S2). In control cells GFP–Lgl1^{WT} localized mainly at the leading edge of the cell (Fig. 3A and supplementary material Fig. S2), whereas in aPKCζ$^{-/-}$ cells GFP–Lgl1^{WT} was confined to the cell cortex, forming a shell-like structure around the cell (Fig. 3B and supplementary material Fig. S2). GFP–Lgl1^{Ala} behaved similarly to GFP–Lgl1^{WT} in aPKCζ$^{-/-}$ cells, forming a sphere around the cell cortex (Fig. 3B and supplementary material Fig. S2). The effects of the absence of aPKCζ on the localization of GFP–Lgl1^{WT} thus resembled those observed with GFP–Lgl1^{Ala}.

In contrast, GFP–Lgl1^{Asp} expressed by control cells was completely diffuse, with the protein distributed throughout the cytoplasm. F-actin staining showed that GFP–Lgl1^{Asp} did not reach the lamellipodium (Fig. 3A and supplementary material Fig. S2). These observations were confirmed by quantification of the fluorescence intensity of GFP–Lgl1 phospho-mutants from the leading edge of the cell towards its center (Fig. 3C,D). The fluorescence intensity patterns of GFP–Lgl1^{WT} and F-actin were similar with maximum fluorescence at the cell edge (Fig. 3C). The fluorescence intensity of GFP–Lgl1^{Ala} in control cells, as well as GFP–Lgl1^{WT} in aPKCζ$^{-/-}$ cells, was higher than that of GFP–Lgl1^{WT} in control cells, demonstrating the concentration of this protein at the cell cortex (Fig. 3C,D). In contrast, GFP–Lgl1^{Asp} fluorescence intensity was much lower than that of GFP–Lgl1^{WT}, further demonstrating the diffusible behavior of this protein (Fig. 3C). These results thus suggest that phosphorylation of Lgl1 by aPKCζ plays an important role in the cellular localization of Lgl1. Interestingly, in cells expressing GFP–Lgl1^{Ala}, or in aPKCζ$^{-/-}$ cells expressing GFP–Lgl1^{WT}, F-actin formed a shell-like structure similar to Lgl1^{Ala}, and in cells expressing GFP–Lgl1^{Asp}, F-actin and GFP–Lgl1^{Aap} did not localized to the lamellipodium, indicating that the state of Lgl1 phosphorylation might also affect the cellular localization of F-actin.

Lgl1 phosphorylation by aPKCζ affects the association of Lgl1 and NMII-A with the cytoskeleton

To further study the role of Lgl1 phosphorylation on its cellular localization, we determined the amount of GFP–Lgl1 phospho-mutants associated with the cytoskeleton using a Triton X-100 solubility assay. A higher percentage of GFP–Lgl1^{WT} was associated with the cytoskeleton in the absence of aPKCζ than in control cells (36% versus 27%; Fig. 4A). Similarly, expression of the unphosphorylated form of Lgl1, GFP–Lgl1^{Ala} in control cells resulted in higher cytoskeletal association than with GFP–Lgl1^{WT} (34% versus 27%, Fig. 4A). The phosphomimetic form of Lgl1, GFP–Lgl1^{Asp}, showed less association with the cytoskeleton than GFP–Lgl1^{WT} (20% versus 27%, Fig. 4A). Together, these results indicate that Lgl1 phosphorylation by aPKCζ regulates its interaction with the cytoskeleton, thus affecting its cellular localization. These findings are consistent with previous reports that *Drosophila* Lgl dissociates from the cytoskeleton on phosphorylation by aPKC (Betschinger et al., 2005).

Journal of Cell Science (2014) 127, 295–304 doi:10.1242/jcs.127357

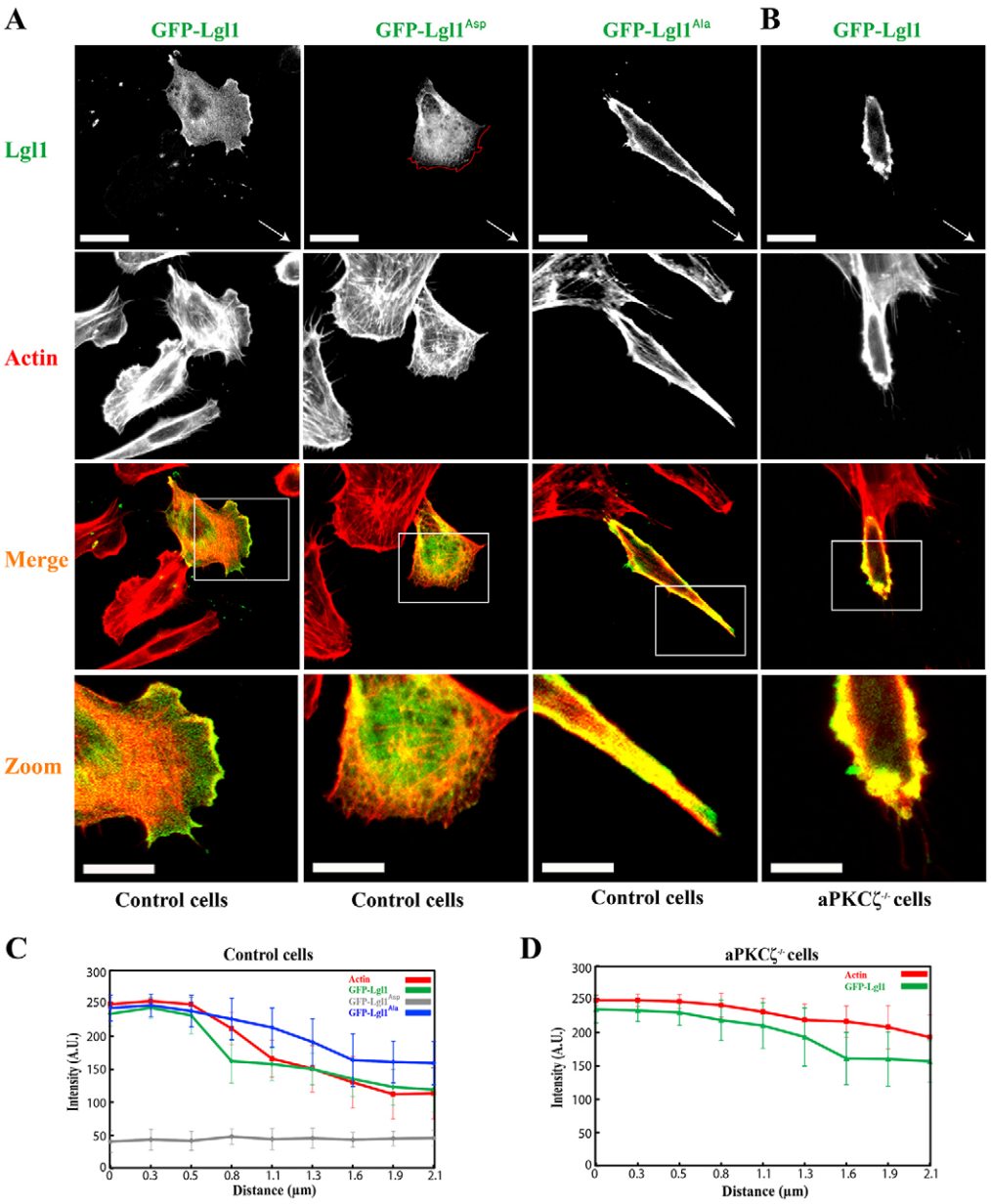

Fig. 3. Phosphorylation of Lgl1 affects its cellular localization. Control cells transfected with GFP–Lgl1^{WT}, GFP–Lgl1^{Ala} or GFP–Lgl1^{Asp} (A) and aPKCζ$^{-/-}$ cells transfected with GFP–Lgl1 (B) were seeded on coverslips, subjected to a scratch wound assay and stained for F-actin using Rhodamine–phalloidin. The leading edge of the cell, as determined by F-actin staining, is indicated by a red line in the GFP–Lgl1^{Asp} column. White arrows indicate the direction of cell migration. The cells were visualized using inverted confocal microscopy. Scale bars: 20 μm (Lgl1); 10 μm (zoom). (C,D) Quantification of fluorescence intensity of GFP–Lgl1 phospho-mutants and F-actin in control cells (C) and in aPKCζ$^{-/-}$ cells (D). Measurements were taken from the cell edge (0 μm) towards the cell center (2 μm). F-actin in C was quantified in cells expressing GFP–Lgl1^{WT}. The values are the means ± s.d. of $n \geq 15$ cells for each condition. The experiment was repeated at least three times with similar results. A.U., arbitrary units.

Because Lgl1 affects the cellular localization of NMII-A (Dahan et al., 2012), we studied the effect of the expression of phospho-Lgl1 mutants on the association of NMII-A with the cytoskeleton. Overexpression of GFP–Lgl1^{WT} reduced NMII-A association with the cytoskeleton compared to control cells (32.6% versus 41.6%, Fig. 4B). Expression of GFP–Lgl1^{Ala} in control cells resulted in a further decrease in the association of NMII-A with the cytoskeleton (23.5% versus 41.6%, Fig. 4B). These results indicate that Lgl1 phosphorylation affects the solubility properties of NMII-A, possibly by regulating NMII-A filament assembly.

Lgl1 exists in two distinct complexes *in vivo* that are affected by Lgl1 phosphorylation

Lgl1 forms multiprotein polarity complex with Par6α and aPKC (Plant et al., 2003). To begin understanding the effect of Lgl1 phosphorylation on the regulation of NMII-A filament assembly, we tested whether Lgl1 exists in a complex with Par6α, aPKCζ and NMII-A. HEK293T cells were co-transfected with GFP-Lgl1^{WT} and HA-Par6α and subjected to co-immunoprecipitation assays using anti-NMII-A, anti-GFP anti-HA or anti-aPKCζ-specific antibodies. Lgl1 immunoprecipitates contained Par6α and aPKCζ as well as NMII-A (Fig. 5A,B). However, Par6α immunoprecipitates contained Lgl1 and aPKCζ but not NMII-A (Fig. 5A,B). Similarly, NMII-A immunoprecipitates contained Lgl1 but not Par6α or aPKCζ (Fig. 5A,B). Thus, Lgl1 forms two distinct complexes *in vivo*, Lgl1–NMII-A and Lgl1–Par6α–aPKCζ.

To study the effect of Lgl1 phosphorylation on its interaction with Par6α and aPKCζ, we examined the ability of Lgl1 C-terminal phospho-mutant protein fragments to bind to endogenous aPKCζ obtained from NIH 3T3 a cell extract, and to expressed Par6α obtained from the HEK293T cell line transfected with HA-Par6α. Only traces of endogenous aPKCζ and HA–Par6α co-precipitated with MBP–Lgl1-C^{Asp}, whereas MBP–Lgl1-C^{WT} and MBP–Lgl1-C^{Ala} co-precipitated with endogenous aPKCζ and HA–Par6α (Fig. 5C,D). These results

Journal of Cell Science (2014) 127, 295–304 doi:10.1242/jcs.127357

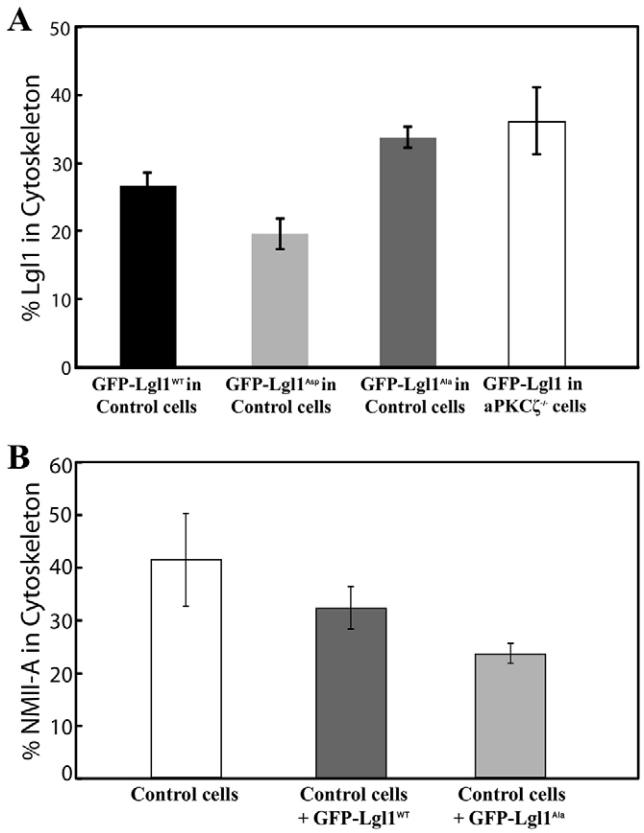

Fig. 4. Phosphorylation of Lgl1 affects its association with acto-NMIIA cytoskeleton. (A) aPKCζ$^{-/-}$ and control cells expressing GFP–Lgl1^{WT} and control cells expressing GFP–Lgl1^{Asp} or GFP–Lgl1^{Ala} were subjected to a Triton X-100 solubility assay and the percentage of Lgl1 phospho-mutants in the insoluble fractions was determined. Values are the means ± s.d. from four independent experiments subjected to two-tailed, two-sample, unequal-variance Student's *t*-test: P=0.002 for GFP–Lgl1^{WT} in control cells versus GFP–Lgl1^{Asp} in control cells; P=0.0002 for GFP–Lgl1^{WT} in control cells versus GFP-Lgl1^{Ala} in control cells; and P=0.01 for GFP–Lgl1^{WT} in control cells versus GFP–Lgl1 in aPKCζ$^{-/-}$ cells. (B) Control cells expressing GFP–Lgl1^{WT} or GFP–Lgl1^{Ala} were subjected to a Triton X-100 solubility assay, and the percentages of NMII-A in the insoluble fractions were determined. Values are the means ± s.d. from three independent experiments subjected to two-tailed, two-sample, unequal-variance Student's *t*-test: P=0.02 for %NMII-A in cytoskeleton in control cells versus %NMII-A in cytoskeleton in control cells+GFP–Lgl1^{WT}; P=0.0006 for %NMII-A in cytoskeleton in control cells versus %NMII-A in cytoskeleton in control cells+GFP–Lgl1^{Ala}; and P=0.04 for %NMII-A in cytoskeleton in control cells+GFP–Lgl1^{WT} versus %NMII-A in cytoskeleton in control cells+GFP–Lgl1^{Ala}.

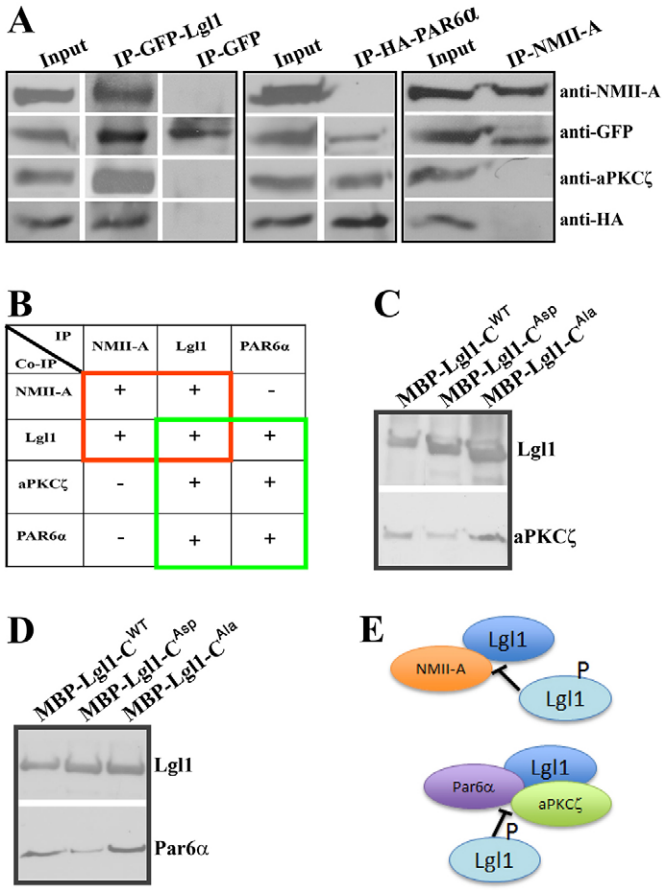

Fig. 5. Lgl1 exists in two distinct complexes *in vivo*. (A) HEK293T cells were co-transfected with GFP-Lgl1 and HA-Par6α constructs and subjected to a co-immunoprecipitation assay using anti-NMII-A, anti-GFP or anti-HA-specific antibodies. The immunoprecipitated proteins were analyzed by immunoblotting with antibodies specific to NMII-A, GFP, aPKCζ and HA. (B) Summary of Lgl1 co-immunoprecipitation with NMII-A, Par6α and aPKCζ. Red frame represents the Lgl1–NMIIA complex and green frame the Lgl1–aPKCζ–Par6α complex. (C) Lgl1 C-terminal phospho-mutant protein fragments were incubated with NIH 3T3 cell lysate and subjected to a pull-down assay. The proteins were detected by immunoblotting with antibodies against Lgl1 and endogenous aPKCζ. (D) Cell extracts from HEK293T cells that were transfected with HA–Par6α were subjected to pull-down assay with Lgl1 C-terminal phospho-mutant protein fragments. The precipitated proteins were analyzed by immunoblotting with antibodies against Lgl1 and HA. (E) A model depicting the effect of Lgl1 phosphorylation on the formation of the two distinct complexes, Lgl1–NMIIA and Lgl1–Par6α–aPKCζ. Unphosphorylated Lgl1 forms a complex with NMII-A and Lgl1-Par6α–aPKCζ. On phosphorylation by aPKCζ, Lgl1 undergoes conformational changes that prevents it binding to NMII-A as well as to Par6α–aPKCζ.

indicate that Lgl1 phosphorylation by aPKCζ inhibits its interaction with aPKCζ and Par6α, as well as NMII-A (Fig. 5E).

aPKCζ and NMII-A compete for binding to Lgl1

Because Lgl1 forms two distinct complexes it is possible that Lgl1 does not bind to aPKCζ and NMII-A concurrently. Hence, we tested whether aPKCζ and NMII-A bind to the same site on Lgl1. Lgl1 C-terminal fragments with different deletions (Fig. 1A) were incubated with endogenous aPKCζ in a cell extract obtained from NIH 3T3 cells, and subjected to a pull-down assay. A Lgl1 fragment containing residues 615–1036 [MBP–Lgl1-C$^{(615–1036)}$] bound to endogenous aPKCζ, whereas a Lgl1 fragment containing residues 678–1036 [MBP–Lgl1-C$^{(678–1036)}$] did not (Fig. 6A). This indicated that the domain of Lgl1 interacting with aPKCζ lay within residues 615–678. This region contains the Lgl1 domain mediating its interactions with NMII-A (residues 645–677) (Dahan et al., 2012). To determine whether this domain also mediates the interaction of Lgl1 with aPKCζ, we tested the ability of MBP–Lgl1-C$^{\Delta MBD}$, which lacks the NMII-A-binding site, to bind endogenous aPKCζ. As shown in Fig. 6A, MBP–Lgl1-C$^{\Delta MBD}$ did not bind the endogenous aPKCζ, indicating that aPKCζ and NMII-A bind to Lgl1 in the same domain.

We next tested whether aPKCζ competes with NMII-A for interaction with Lgl1. Proteins that belong to the PKC family are regulated by auto-inhibition through their pseudosubstrate domain, with the pseudosubstrate site binding to the substrate-binding

Journal of Cell Science (2014) 127, 295–304 doi:10.1242/jcs.127357

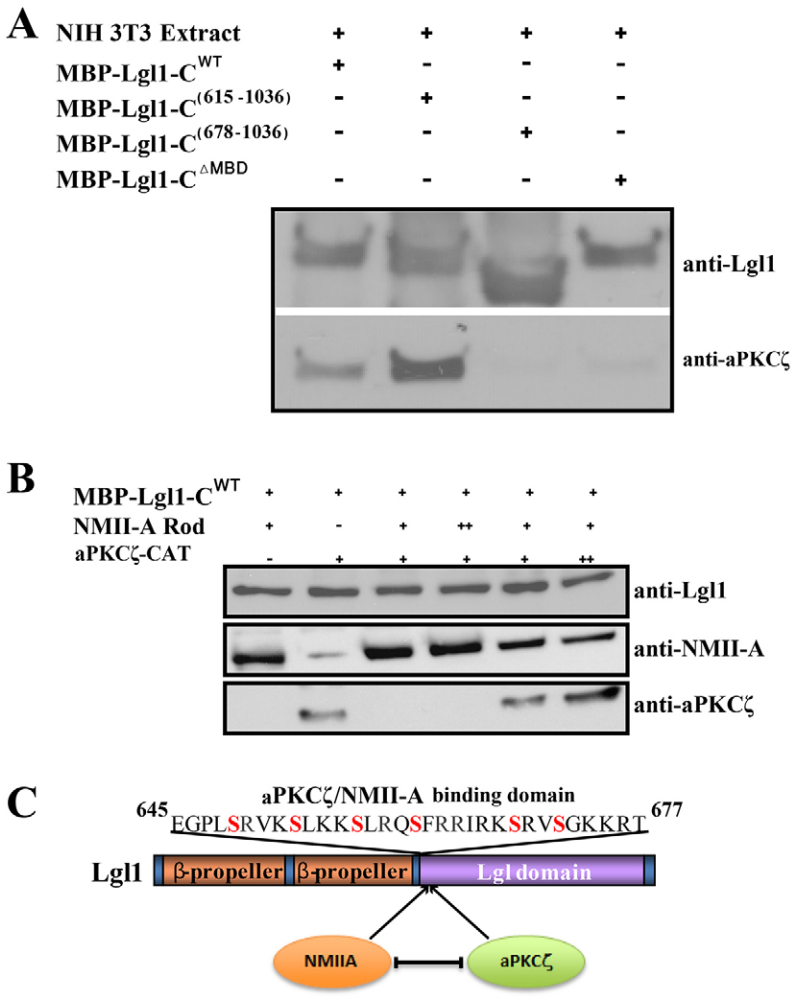

Fig. 6. NMII-A and aPKCζ compete for binding to Lgl1. (A) MBP–Lgl1-C^{WT} was incubated with NIH 3T3 cell lysate and subjected to a pull-down assay. Proteins were detected by immunoblotting with antibodies against aPKCζ and Lgl1. (B) A competition assay was performed using immobilized MBP–Lgl1-C^{WT}, NMII-A Rod and aPKCζ-CAT. Proteins were analyzed by immunoblotting with antibodies against Lgl1, NMII-A and aPKCζ. '+' and '++' indicate 1:1 and 1:5 molar ratio, respectively, of MBP–Lgl1-C^{WT} to NMII-A Rod or aPKCζ-CAT. (C) Lgl1 binding domain for aPKCζ and summary of the interactions of Lgl1 with NMII-A or aPKCζ. Red Ss indicate serines that are target sites for aPKCζ. Numbers indicate the amino acid positions in the full-length protein.

pocket in the kinase domain (Rosse et al., 2010). We therefore used a recombinant catalytic domain of aPKCζ (aPKCζ-CAT). Preincubation of MBP–Lgl1-C^{WT} with NMII-A Rod at a molar ratio of 1:1 or 1:5 completely inhibited the subsequent binding of aPKCζ-CAT (Fig. 6B). Similarly, preincubation of MBP–Lgl1-C^{WT} with aPKCζ-CAT at a molar ration of 1:1 or 1:5 inhibited the binding of NMII-A Rod to MBP–Lgl1-C^{WT}. These results indicate that aPKCζ and NMII-A show competitive binding to Lgl1 amino acid residues 645–677 (Fig. 6C).

Lgl1, Par6α and aPKCζ form a complex at the leading edge of the cell

Finding that Lgl1 formed a complex with Par6α and aPKCζ led us to examine the localization properties of these polarity proteins in polarized migrating cells. Control cells were transfected with GFP-Lgl1^{WT} or HA-Par6α and subjected to a scratch wound assay to achieve polarized migrating cells. The cellular localizations of GFP–Lgl1^{WT}, HA–Par6α, endogenous aPKCζ and NMII-A were determined. In migrating polarized cells, GFP–Lgl1^{WT} or HA–Par6α colocalized with aPKCζ at the leading edge of the cell (Fig. 7A,B; supplementary material Figs S3 and S4). NMII-A was present in the lamellum but absent from the lamellipodium (Fig. 7A,B; supplementary material Figs S3 and S4) as previously described (Gupton and Waterman-Storer, 2006; Kolega, 1998; Vicente-Manzanares et al., 2007). These observations were confirmed by quantification of the fluorescence intensity of GFP–Lgl1^{WT}, HA–Par6α, aPKCζ and NMII-A from the leading edge of the cell towards its center (Fig. 5C,D). The fluorescence intensity of GFP–Lgl1 or HA–Par6α, and aPKCζ revealed a similar pattern, with maximum fluorescence at the cell edge (Fig. 7C,D). In contrast very little NMII-A was present at the cell edge but rose gradually toward the cell center (Fig. 7C,D). These results confirmed the presence of Lgl1 and Par6α at the leading edge of the cell and their colocalization with aPKCζ, as well as the absence of NMII-A in this region. These results are in agreement with a previous study showing that Lgl1 colocalized with aPKC in migrating murine fibroblast cells (Plant et al., 2003).

DISCUSSION

We recently showed that NMII-A and the tumor suppressor Lgl1 play a central role in the polarization of migrating cells (Dahan et al., 2012). In mammalian cells Lgl1 interacts directly with NMII-A through a negatively charged region on the NMII-A molecule, inhibiting its ability to assemble into a filament. The binding domain of Lgl1 for NMII-A is positively charged and contains the phosphorylation sites for aPKCζ (Dahan et al., 2012). Therefore, we proposed that the interaction between Lgl1 and NMII-A is electrostatic and that phosphorylation of Lgl1 decreases the positive charge of the Lgl1 interacting domain. This would prevent its binding to NMII-A and thereby regulate Lgl1–NMII-A interaction (Dahan et al., 2012). This hypothesis is supported by previous findings that phosphorylation of

Journal of Cell Science (2014) 127, 295–304 doi:10.1242/jcs.127357

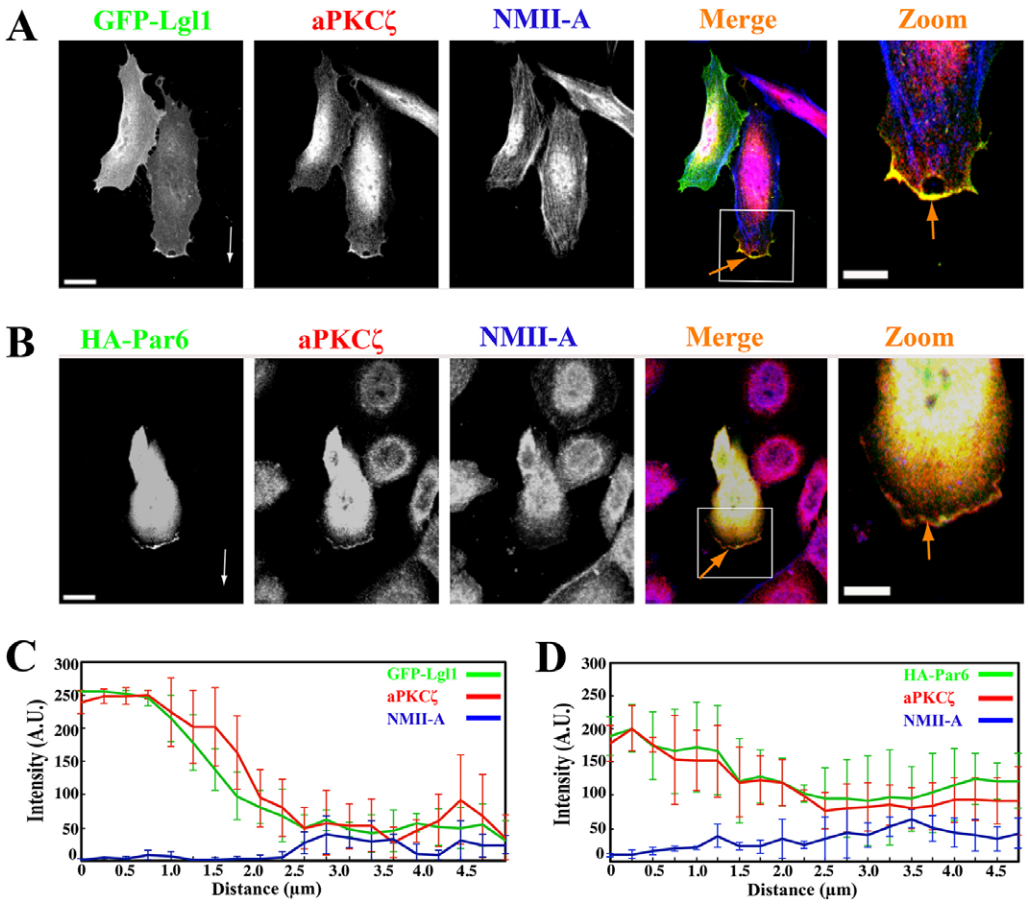

Fig. 7. Lgl1, aPar6α and aPKCζ colocalize at the cell leading edge. Control cells transfected with GFP-Lgl1 (A) or HA-Par6α (B) were seeded on coverslips and subjected to a scratch wound assay, stained for HA–Par6α using HA-specific antibody conjugated to FITC, for NMII-A using a C-terminal-specific antibody conjugated to Cy5, and for aPKCζ with a specific antibody conjugated to Rhodamine. The white box in the merge column indicates the position of the higher magnification shown in the rightmost column. White and orange arrows indicate the direction of cell migration and the colocalization of GFP–Lgl1 or HA–Par6α and aPKCζ, respectively. Scale bars: 20 μm (GFP–Lgl1 and HA–Par6α); 10 μm (Zoom). (C,D) Quantification of fluorescence intensity of GFP–Lgl1, aPKCζ and NMII-A (C) and HA–Par6α, aPKCζ and NMII-A (D) measured from the cell edge (0 μm) towards the cell center (5 μm). The data are means ± s.e.m. of $n \geq 15$ cells. The experiment was repeated at least three times with similar results. A.U., arbitrary units.

Drosophila Lgl dissociates it from the cytoskeleton (Betschinger et al., 2005). Here we confirmed this hypothesis and provided new insights into the mechanism by which Lgl1–NMII-A interaction is regulated by the phosphorylation of Lgl1 by aPKCζ.

Lgl1 and Lgl1^{Ala} but not Lgl1^{Asp} bind to NMII-A both *in vitro* and *in vivo*. These results fit with our findings that in polarized migrating cells the state of Lgl1 phosphorylation determines its localization properties and its association with the cytoskeleton. The phosphorylatable form of Lgl1 localized to the leading edge of the cell, whereas the phosphomimetic form of Lgl1 (Lgl1^{Asp}) diffused throughout the cell and was completely absent from the leading edge. In contrast, the unphosphorylatable form of Lgl1 (Lgl1^{Ala}) was mainly restricted to the cell cortex. These cellular localization properties were also reflected by the degree of association of the various Lgl1 phospho-mutants with the cytoskeleton. These results indicate that phosphorylation of Lgl1 plays a crucial role in its association with the cytoskeleton, as well as in its cellular localization.

Lgl1 phosphorylation also affects the association of NMII-A with the cytoskeleton. Expression of the phosphorylatable form of Lgl1 decreased the amount of NMII-A associated with the cytoskeleton. Expression of the unphosphorylatable form of Lgl1 decreased this further. Lgl1 binding to NMII-A inhibits filament assembly (Dahan et al., 2012) and Lgl1 phosphorylation decreased the interaction between these proteins. We therefore propose that the effect of a decrease in the amount of NMII-A associated with the cytoskeleton because of the expression of Lgl1 or Lgl1^{Ala} mirrors the increased amounts of non-filamentous NMII-A. The reduction in the amount of NMII-A associated with the cytoskeleton as a result of the expression of Lgl1 and Lgl1^{Ala} is possibly due to the partial phosphorylation of the expressed Lgl1 by endogenous aPKCζ.

aPKCζ is part of the polarity complex Par6α–Par3 involved in establishing the apical-basal polarity of epithelial cells (Bilder, 2004; Gao and Macara, 2004; Knust and Bossinger, 2002). A direct interaction between basolateral Lgl and the apical aPKC–Par6 complex has been demonstrated in *Drosophila* and mammalian epithelial cells (Betschinger et al., 2003; Hutterer et al., 2004; Plant et al., 2003; Yamanaka et al., 2003). *Drosophila* Lgl phosphorylation by aPKC is required for the exclusion of Lgl from the apical region in epithelial cells (Betschinger et al., 2003; Hutterer et al., 2004; Müsch et al., 2002; Yamanaka et al., 2003). In a genetic study in *Drosophila*, reduction in aPKC levels suppressed the development of Lgl mutant phenotypes, such as cell polarity defects and tumorigenesis (Rolls et al., 2003). Further, studies using *Drosophila* or *Xenopus* embryo indicated that mutual inhibition between apical aPKC and basolateral Lgl is important in maintaining epithelial membrane polarity (Chalmers et al., 2005; Hutterer et al., 2004). These observations suggest that an antagonistic interaction of Lgl with apical Par3–aPKC–Par6 complex is important for the development of polarized membrane domains in epithelial cells. Here we have shown that aPKCζ is necessary for proper cellular localization of Lgl1. The cellular localization of Lgl1 in aPKCζ$^{-/-}$ cells was aberrant, similar to that of unphosphorylatable Lgl1, indicating the important role of aPKCζ in the regulation of Lgl1.

Finally, our findings indicate that *in vivo* Lgl1 exists in two distinct complexes, Lgl1–NMII-A and Lgl1–Par6α–aPKCζ that are affected by the state of Lgl1 phosphorylation. The formation of two

Journal of Cell Science (2014) 127, 295–304 doi:10.1242/jcs.127357

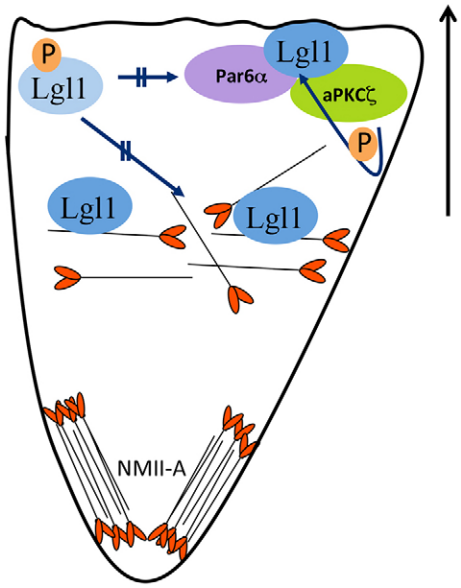

Fig. 8. A model summarizing the role of the Lgl1 complexes, Lgl1–NMII-A and Lgl1–Par6α–aPKCζ, in establishing the polarity of migrating cells, and the role of Lgl1 regulation by aPKCζ phosphorylation (see text for further details). The large black arrow indicates the direction of migration.

discrete complexes is explained by our finding that NMII-A and aPKCζ compete to bind to the same region on Lgl1. This behavior may ensure the cellular localization of the two complexes to different cellular compartments, thereby establishing front–rear polarization in migrating cells. Indeed, the complex Lgl1–Par6α–aPKCζ resides in the leading edge, a region that is not occupied by NMII-A. We propose that Lgl1 in the leading edge is in the unphosphorylated state and therefore forms a complex with Par6α–aPKCζ in this region. It is possible that non-filamentous NMII-A forms a complex with unphosphorylated Lgl1 at the lamellipodium, preventing NMII-A from assembling into filaments, thus allowing polymerization of F-actin in that region. In contrast, filamentous NMII-A that is not bound to Lgl1 is found in the lamellum where, along with F-actin, it forms the stress fibers required for detachment of a migrating cell. It is plausible that we did not detect the Lgl1–NMII-A in the lamellipodium because of the formation of Lgl1 and NMII-A-monomer complexes that are too small to detect.

Based on all the results presented here, we propose a model for the role of Lgl1–NMIIA and Lgl1–Par6α–aPKCζ in establishing front–rear polarization in migrating cells (Fig. 8). In migrating polarized cells Lgl1 resides at the leading edge of the cell in a complex with Par6α–aPKCζ, and it is this complex that defines the leading edge. In the lamellipodium Lgl1 binds to NMII-A but not to aPKCζ, inhibiting NMII-A filament assembly. These events allow the cell to polymerize F-actin to move the cell forward. According to our model, Lgl1 is absent from the rear part of the cell, allowing NMII-A to assemble into filaments to enable cell retraction.

MATERIALS AND METHODS

The proteins used for this study were human NMII-A, mouse Lgl1 and mouse-Par6α, accession numbers NM_002473, NM_005964, NM_008502 and NM_001047436, respectively.

Cell lines and culture conditions

Control and aPKCζ$^{-/-}$ primary embryo fibroblasts were kindly provided by Dr Jorge Moscat (Sanford-Burnham Medical Research Institute, La Jolla). Control and aPKCζ$^{-/-}$ primary embryo fibroblasts, mouse embryonic fibroblast NIH 3T3 and HEK293T cell lines were maintained in high glucose DMEM supplemented with 2 mM L-glutamine, 10% FCS and antibiotics (100 U/ml penicillin, 100 mg/ml streptomycin and 1:100 Biomyc3 anti-mycoplasma antibiotic solution; Biological Industries, Beit HaEmek, Israel). Cells were grown at 37℃ in a humidified atmosphere of 5% CO_2 and 95% air.

Antibodies

Antibodies specific for the C-terminal region of mouse NMII-A were a kind gift from Dr R. S. Adelstein (NIH/NHLBI). Antibodies specific for the C-terminal region of human NMII-A were generated in rabbits according to the method of Phillips et al. (Phillips et al., 1995). Recombinant GFP antibodies were prepared in rabbits as described previously (Rosenberg and Ravid, 2006). Specific antibodies for the C- and N-terminal domains of Lgl1 were generated in rabbit using the peptides DTTLDTTGDVTVEDVKD and DDYRCGKALGPVESLQ, respectively (Dahan et al., 2012). Anti-mouse monoclonal β-actin antibodies were purchased from Sigma-Aldrich and anti-rat monoclonal HA antibodies from Roche Diagnostics Corporation (Basel, Switzerland). Anti-mouse monoclonal aPKCζ antibodies were purchased from Santa Cruz Biotechnology.

Preparation of plasmid constructs

Mouse Lgl1 and pMBP-3 (Sheffield et al., 1999) were kindly provided by Dr T. Pawson (Mount Sinai Hospital, Toronto, Canada), and Dr P. Sheffield (University of Virginia, Charlottesville, Virginia, USA), respectively. pMBP-Lgl1-C, pMBP-Lgl1(678–1036), pMBP-Lgl1(615–1036) and pMBP-Lgl1-CΔ(645–677) were created as described previously (Dahan et al., 2012). To create pGST-Lgl1, Lgl1 in a pCMV5 vector was digested with *Bam*HI and the fragment was inserted into a pGEX-3X vector that was digested with *Bam*HI. GST–Lgl1^{Ala} was created by replacing the conserved serine residues at positions 658, 662 and 669 in the Lgl1 protein with alanine residues using the QuikChange site-directed mutagenesis kit (Stratagene) with the following primer 5′-CGGGTGAAGGCCCTCAAGAAGGCACTGAGACAGGCATTCC-GGC-3′. The mutations were verified by DNA sequencing (Center for Genomic Analysis, The Hebrew University, Jerusalem). GST-Lgl1^{Asp} was created with a series of mutagenesis reactions by substituting the conserved serine residues at positions 658, 662 and 669 in the Lgl1 protein with aspartate residues using the QuikChange Site-directed mutagenesis kit (Stratagene) with the following primers 5′-GAAGTCA-CTGAGACAGGATTTCCGGCGAATCCGCAAGAG-3′ for substitution of the serine residue in position 669 and 5′-CCACTGTCACGGGT-GAAGGACCTCAAGAAGGACCTGAGACAGG-3′ for substitution of serine residues in positions 658 and 662. The mutations were confirmed by DNA sequencing (Center for Genomic Analysis, The Hebrew University, Jerusalem). To create pGFP-Lgl1, GFP-Lgl1^{Ala} and GFP-Lgl1^{Asp}, pGST-Lgl1 were digested with *Bam*HI and the fragment was ligated into pGFP-C2 that was digested with *Bam*HI. To create pMBP-Lgl1^{Ala} and pMBP-Lgl1^{Asp} the vectors GFP-Lgl1^{Ala} and GFP-Lgl1^{Asp} were digested with *Bam*HI and the fragments were inserted into pMBP-3 digested with *Bam*HI. To create pMBP-Lgl1-C^{Ala} and pMBP-Lgl1-C^{Asp}, the vectors pMBP-Lgl1^{Ala} and pMBP-Lgl1^{Asp} were digested with *Kpn*I and the fragments were inserted into different pMBP-3 plasmids digested with *Kpn*I. Par6α was kindly donated by Dr T. Pawson. To create pGFP-Par6α, Par6α in the pCDN3 vector was digested with Cfr42I and *Eco*RI and the fragment was inserted into pGFP-2 digested with Cfr42I and *Eco*RI. HA fused to Par6α was created by removing the GFP tag from GFP-Par6α using *Nhe*I and *Hin*dIII and the following synthetic primers coding for the HA tag 5′-CTAGCATGGATTACCCATACGATGTTCC-AGATTACGCTCGA-3′ were subsequently ligated into the gap. NMII-A Rod fragment in pET21 that encodes for 480 residues from the NMII-A heavy chain C-terminus (SwissProt P35579, amino acids 1480–1960) with the addition of two amino acids on the N-terminus was prepared as previously described (Ronen and Ravid, 2009). Histidine-tagged aPKCζ-CAT was kindly provided by Dr Yehiel Zick (Weizmann Institute, Rehovot, Israel).

Journal of Cell Science (2014) 127, 295–304 doi:10.1242/jcs.127357

Bacterial expression and purification of recombinant proteins

MBP-Lgl1-C constructs were transformed into *Escherichia coli* BL21-CodonPlus(DE3)-RIL, obtained from Dr Tsafi Danieli, (Hebrew University of Jerusalem, Israel) and the bacteria were grown in 100 ml lysogeny broth (LB) with 50 μg/ml ampicillin at 37℃ to and $OD_{600}=0.5$. 0.1 mM IPTG was then added and the bacteria were grown for an additional 3 hours at 25℃. The bacteria were pelleted at 12,000 ***g*** at 4℃ for 20 minutes and the pellets frozen at −20℃. The bacterial pellet was dissolved in 4 ml MBP buffer [20 mM Tris-HCl pH 7.5, 5 mM $MgCl_2$, 150 mM NaCl, 1 mM dithiothreitol (DTT) and 0.1 mM phenylmethylsulfonyl fluoride (PMSF)] and 1 mg/ml lysozyme and incubated on ice for 15 minutes. The lysate was sonicated for 5× 10 seconds (Misonix Microson-Ultrasonic cell disruptor) and centrifuged at 16,000 ***g*** at 4℃ for 20 minutes. 500 μl of 50% amylose beads slurry (New England BioLabs) was washed twice with MBP buffer, added to the bacterial lysate and incubated at 4℃ for 2 hours on a rotator, followed by three washes with MBP buffer. Expression and purification of NMII-A Rod was carried out according to Straussman et al. (Straussman et al., 2007). Histidine-tagged aPKCζ-CAT was expressed and purified according to the manufacturer's instructions (Thermo Scientific, Rockford, IL). The concentrations of the MBP–Lgl1-C proteins bound to amylase beads, NMII-A Rod and aPKCζ-CAT were determined by comparing the densitometry of the band of a sample of each protein on Coomassie-Blue-stained polyacrylamide gels to known amounts of BSA samples on the same gel.

Pull-down and competition assays

3 μg MBP–Lgl1-C phospho-mutant protein fragments immobilized on amylose beads in 500 μl CHAPS buffer was incubated with 1 μg NMII-A Rod at 4℃ for 2 hours on a rotator. Bound proteins were washed three times in CHAPS buffer and resolved by 10% SDS-PAGE. For competition assays, MBP–Lgl1-C^{WT} immobilized on amylose beads in 500 μl CHAPS buffer was incubated with NMII-A Rod fragment (1:1 and 1:5 molar ratios) at 4℃ for 2 hours. After washing with CHAPS buffer, aPKCζ-CAT (1:1 and 1:5 molar ratios) was added and incubated at 4℃ for 2 hours on a rotator. For the reciprocal experiment aPKCζ-CAT was preincubated with immobilized MBP–Lgl1-C^{WT}. After washing with CHAPS buffer, NMII-A Rod was added. Bound proteins were resolved by SDS-PAGE analysis and then immunoblotted with anti-Lgl1, anti-NMII-A and anti-aPKCζ.

Inhibition of NMII-A filament assembly by MBP–Lgl1-C phospho-mutant protein fragments

Maltose (0.1 M) was added to 1.2 ml MBP–Lgl1 C-terminal phospho-mutant protein fragments immobilized on amylose beads, which were then incubated on a rotator for 1 hour at 4℃ and centrifuged at 6000 ***g*** at 4℃ for 2 minutes. The supernatants were dialyzed against MBP buffer containing 1 mM DTT and 0.1 mM PMSF. Protein concentrations were determined as described in Materials and Methods. MBP–Lgl1-C fusion proteins at 3–6 μM were added to monomeric NMII-A Rod in 20 mM Tris-HCl (pH 7.5), 600 mM NaCl, 5 mM EDTA, 1 mM DTT, dialyzed against 10 mM phosphate buffer, pH 7.5, 2 mM $MgCl_2$ and 150 mM NaCl for 4 hours at 4℃. The protein mix was centrifuged in a TL-100 ultracentrifuge (Beckman Coulter, Fullerton, CA) at 100,000 ***g***, at 4℃ for 1 hour, and the supernatant and pellet were separated on 10% SDS-PAGE. The gels were stained with Coomassie Brilliant Blue, scanned, and quantified using the densitometry program Fujifilm ImageGauge V.

Binding of MBP–Lgl1-C phospho-mutant protein fragments to cell extract proteins

NIH 3T3 cells were grown on 60 mm plates to 60–80% confluency and lysed with ice-cold CHAPS buffer (50 mM Tris-HCl pH 7.5, 150 mM NaCl, 5 mM EDTA, 5 mM EGTA, 1% CHAPS, 1 mM DTT) and protease inhibitor cocktail (Sigma-Aldrich). Lysates were transferred to Eppendorf tubes, incubated on ice for 15 minutes and centrifuged at 16,000 ***g*** at 4℃ for 15 minutes. The supernatants were incubated at 4℃ with MBP–Lgl1-C phospho-mutant protein fragments bound to amylase beads, followed by three washes with CHAPS buffer. Samples were separated on 7% SDS-PAGE, and western blotting was performed using anti-mouse NMII-A, anti-aPKCζ and anti-Lgl1 antibodies.

Co-immunoprecipitation and western blotting

pGFP-Lgl1 phospho-mutants or pGFP-$Lgl1^{WT}$ and HA-Par6α were co-transfected into an ∼70% confluent HEK293T cell line on 100-mm plates using polyethylenimine (PEI) transfection reagent (Sigma-Aldrich). Forty-eight hours after transfection the cells were washed three times with ice-cold PBS and lysed with 1 ml NP-40 buffer (10 mM Tris-HCl, pH 8, 1 mM EDTA, 100 mM NaCl, 1 mM DTT and 0.5% NP-40) containing protease inhibitor cocktail (Sigma-Aldrich). Cells were then sonicated, incubated for 15 minutes on ice, and centrifuged at 25,000 ***g*** at 4℃ for 15 minutes. 50 μl of the supernatants were used for input control, the remainder of the supernatants were transferred to fresh tubes containing protein A agarose beads (Pierce, Rockford, IL) coupled to anti-human NMII-A or anti-GFP antibodies and protein G agarose beads (Pierce, Rockford, IL) coupled to anti-HA antibodies, rotated at 4℃ for 2 hours, followed by four washes with NP-40 buffer. Samples were dissolved in SDS-PAGE sample buffer, separated using 7% SDS-PAGE and subjected to western blotting using anti-human NMII-A, anti-GFP, anti-aPKCζ and anti-HA antibodies.

Scratch wound assay and confocal microscopy

Control cells (6×10^5) were transfected with GFP-$Lgl1^{WT}$, GFP-$Lgl1^{Ala}$ or GFP-$Lgl1^{Asp}$ or HA-Par6α and 6×10^5 aPKCζ$^{-/-}$ cells were transfected with GFP-$Lgl1^{WT}$ using linear polyethylenimine (L-PEI) transfection reagent (PolyScience). Cells were then seeded on coverslips coated with 27 μg/ml collagen type I (Sigma-Aldrich). At 48 hours post-transfection three parallel scratches were made with a small pipette tip, and the cells were washed twice in PBS to remove cell debris. High-glucose DMEM medium was then added, and cells were incubated for 7 hours, after which they were washed three times with PBS and fixed for 20 minutes in 1.5 ml 3.7% formaldehyde in PBS. aPKCζ$^{-/-}$ and control cell lines without transfection were treated in the same way and were immunostained with anti-mouse NMII-A antibody and secondary antibody conjugated to Cy5. aPKCζ was stained with anti-mouse monoclonal aPKCζ antibodies, HA–Par6α was stained with anti-rat monoclonal HA antibodies. F-actin was stained with Rhodamine–phalloidin as described previously (Ronen and Ravid, 2009). Cells were viewed using confocal microscopy.

Triton solubility assay

aPKCζ$^{-/-}$ (6×10^5) and control cells (8×10^5) were transfected with GFP–Lgl1 phospho-mutant proteins using linear polyethylenimine (L-PEI) transfection reagent (PolyScience). Both transfected and untransfected aPKCζ$^{-/-}$ and control cells were seeded on 30 mm dishes, washed twice with 1 ml PBS and lysed by adding 200 μl PEM buffer (100 mM PIPES pH 6.9, 1 mM $MgCl_2$, 1 mM EGTA) with 1% Triton-X-100 and a protease inhibitor mix (Sigma). This was followed by incubation on ice for 5 minutes. The Triton-soluble fractions were collected from the plates and centrifuged for 5 minutes at 16,000 ***g*** to remove the remnants of the insoluble fraction. 100 μl of supernatant was removed to fresh tubes, 25 μl of 5× SDS-PAGE sample buffer was added, and the tubes were boiled for 5 minutes at 100℃. The insoluble fraction was washed once with 300 ml PEM buffer, then 120 μl SDS-PAGE sample buffer was added to the plates and the insoluble fraction was collected and boiled for 5 minutes at 100℃. After separation on 8% SDS-PAGE, western blot analysis was performed as described above using anti-mouse NMII-A and anti-Lgl1 antibodies. The western blots were developed using the EZ-ECL Chemiluminescence Detection kit (Biological Industries) and the intensities of the bands were analyzed using Fujifilm ImageGauge V software. In the final calculations of the percentage of the proteins in the soluble fractions, the amount of the proteins in the Triton-soluble fraction was corrected by a factor of two and the intensity of proteins in the Triton-soluble fraction was divided by the sum of the intensities of the proteins in the Triton-soluble and -insoluble fractions.

Acknowledgements
We thank Tony Pawson (Mount Sinai Hospital, Toronto, Canada) for Lgl1 and Par constructs and Jorge Moscat (Sanford-Burnham Medical Research Institute, La Jolla) for aPKCζ knockout MEF cells. S.R. holds the Dr Daniel G. Miller Chair in Cancer Research.

Competing interests
The authors declare no competing interests.

Author contributions
I.D. and D.P. performed the experiments; E.C.-K. assisted with the experiments described in Figures 1 and 5; S.R. designed the experiments, analyzed the data, designed the figures, wrote the manuscript and obtained funding for this study.

Funding
This study was supported by the Israel Science Foundation [grant number 1174/12 to S.R.]; and the Israel Cancer Research Fund [to S.R.]; and the Canadian Friends of the Hebrew University [to I.D.].

Supplementary material
Supplementary material available online at
http://jcs.biologists.org/lookup/suppl/doi:10.1242/jcs.127357/-/DC1

References

Betschinger, J., Mechtler, K. and Knoblich, J. A. (2003). The Par complex directs asymmetric cell division by phosphorylating the cytoskeletal protein Lgl. *Nature* **422**, 326-330.
Betschinger, J., Eisenhaber, F. and Knoblich, J. A. (2005). Phosphorylation-induced autoinhibition regulates the cytoskeletal protein Lethal (2) giant larvae. *Curr. Biol.* **15**, 276-282.
Bilder, D. (2004). Epithelial polarity and proliferation control: links from the Drosophila neoplastic tumor suppressors. *Genes Dev.* **18**, 1909-1925.
Bilder, D. and Perrimon, N. (2000). Localization of apical epithelial determinants by the basolateral PDZ protein Scribble. *Nature* **403**, 676-680.
Bilder, D., Li, M. and Perrimon, N. (2000). Cooperative regulation of cell polarity and growth by Drosophila tumor suppressors. *Science* **289**, 113-116.
Cai, Y., Biais, N., Giannone, G., Tanase, M., Jiang, G., Hofman, J. M., Wiggins, C. H., Silberzan, P., Buguin, A., Ladoux, B. et al. (2006). Nonmuscle myosin IIA-dependent force inhibits cell spreading and drives F-actin flow. *Biophys. J.* **91**, 3907-3920.
Chalmers, A. D., Pambos, M., Mason, J., Lang, S., Wylie, C. and Papalopulu, N. (2005). aPKC, Crumbs3 and Lgl2 control apicobasal polarity in early vertebrate development. *Development* **132**, 977-986.
Conti, M. A. and Adelstein, R. S. (2008). Nonmuscle myosin II moves in new directions. *J. Cell Sci.* **121**, 11-18.
Dahan, I., Yearim, A., Touboul, Y. and Ravid, S. (2012). The tumor suppressor Lgl1 regulates NMII-A cellular distribution and focal adhesion morphology to optimize cell migration. *Mol. Biol. Cell* **23**, 591-601.
Dulyaninova, N. G., Malashkevich, V. N., Almo, S. C. and Bresnick, A. R. (2005). Regulation of myosin-IIA assembly and Mts1 binding by heavy chain phosphorylation. *Biochemistry* **44**, 6867-6876.
Etienne-Manneville, S. (2008). Polarity proteins in glial cell functions. *Curr. Opin. Neurobiol.* **18**, 488-494.
Even-Faitelson, L. and Ravid, S. (2006). PAK1 and aPKCzeta regulate myosin II-B phosphorylation: a novel signaling pathway regulating filament assembly. *Mol. Biol. Cell* **17**, 2869-2881.
Gao, L. and Macara, I. G. (2004). Isoforms of the polarity protein par6 have distinct functions. *J. Biol. Chem.* **279**, 41557-41562.
Golomb, E., Ma, X., Jana, S. S., Preston, Y. A., Kawamoto, S., Shoham, N. G., Goldin, E., Conti, M. A., Sellers, J. R. and Adelstein, R. S. (2004). Identification and characterization of nonmuscle myosin II-C, a new member of the myosin II family. *J. Biol. Chem.* **279**, 2800-2808.
Gupton, S. L. and Waterman-Storer, C. M. (2006). Spatiotemporal feedback between actomyosin and focal-adhesion systems optimizes rapid cell migration. *Cell* **125**, 1361-1374.
Hutterer, A., Betschinger, J., Petronczki, M. and Knoblich, J. A. (2004). Sequential roles of Cdc42, Par-6, aPKC, and Lgl in the establishment of epithelial polarity during Drosophila embryogenesis. *Dev. Cell* **6**, 845-854.
Jay, P. Y., Pham, P. A., Wong, S. A. and Elson, E. L. (1995). A mechanical function of myosin II in cell motility. *J. Cell Sci.* **108**, 387-393.
Kalmes, A., Merdes, G., Neumann, B., Strand, D. and Mechler, B. M. (1996). A serine-kinase associated with the p127-l(2)gl tumour suppressor of Drosophila may regulate the binding of p127 to nonmuscle myosin II heavy chain and the attachment of p127 to the plasma membrane. *J. Cell Sci.* **109**, 1359-1368.
Katsuragawa, Y., Yanagisawa, M., Inoue, A. and Masaki, T. (1989). Two distinct nonmuscle myosin-heavy-chain mRNAs are differentially expressed in various chicken tissues. *Eur. J. Biochem.* **184**, 611-616.
Klezovitch, O., Fernandez, T. E., Tapscott, S. J. and Vasioukhin, V. (2004). Loss of cell polarity causes severe brain dysplasia in Lgl1 knockout mice. *Genes Dev.* **18**, 559-571.
Knust, E. and Bossinger, O. (2002). Composition and formation of intercellular junctions in epithelial cells. *Science* **298**, 1955-1959.
Kolega, J. (1998). Cytoplasmic dynamics of myosin IIA and IIB: spatial 'sorting' of isoforms in locomoting cells. *J. Cell Sci.* **111**, 2085-2095.
Lauffenburger, D. A. and Horwitz, A. F. (1996). Cell migration: a physically integrated molecular process. *Cell* **84**, 359-369.
Leitges, M., Sanz, L., Martin, P., Duran, A., Braun, U., García, J. F., Camacho, F., Diaz-Meco, M. T., Rennert, P. D. and Moscat, J. (2001). Targeted disruption of the zetaPKC gene results in the impairment of the NF-kappaB pathway. *Mol. Cell* **8**, 771-780.
Mitchison, T. J. and Cramer, L. P. (1996). Actin-based cell motility and cell locomotion. *Cell* **84**, 371-379.
Murakami, N., Kotula, L. and Hwang, Y.-W. (2000). Two distinct mechanisms for regulation of nonmuscle myosin assembly via the heavy chain: phosphorylation for MIIB and mts 1 binding for MIIA. *Biochemistry* **39**, 11441-11451.
Müsch, A., Cohen, D., Yeaman, C., Nelson, W. J., Rodriguez-Boulan, E. and Brennwald, P. J. (2002). Mammalian homolog of Drosophila tumor suppressor lethal (2) giant larvae interacts with basolateral exocytic machinery in Madin-Darby canine kidney cells. *Mol. Biol. Cell* **13**, 158-168.
Ohshiro, T., Yagami, T., Zhang, C. and Matsuzaki, F. (2000). Role of cortical tumour-suppressor proteins in asymmetric division of Drosophila neuroblast. *Nature* **408**, 593-596.
Peng, C. Y., Manning, L., Albertson, R. and Doe, C. Q. (2000). The tumour-suppressor genes lgl and dlg regulate basal protein targeting in Drosophila neuroblasts. *Nature* **408**, 596-600.
Phillips, C. L., Yamakawa, K. and Adelstein, R. S. (1995). Cloning of the cDNA encoding human nonmuscle myosin heavy chain-B and analysis of human tissues with isoform-specific antibodies. *J. Muscle Res. Cell Motil.* **16**, 379-389.
Plant, P. J., Fawcett, J. P., Lin, D. C., Holdorf, A. D., Binns, K., Kulkarni, S. and Pawson, T. (2003). A polarity complex of mPar-6 and atypical PKC binds, phosphorylates and regulates mammalian Lgl. *Nat. Cell Biol.* **5**, 301-308.
Ridley, A. J., Schwartz, M. A., Burridge, K., Firtel, R. A., Ginsberg, M. H., Borisy, G., Parsons, J. T. and Horwitz, A. R. (2003). Cell migration: integrating signals from front to back. *Science* **302**, 1704-1709.
Rolls, M. M., Albertson, R., Shih, H. P., Lee, C. Y. and Doe, C. Q. (2003). Drosophila aPKC regulates cell polarity and cell proliferation in neuroblasts and epithelia. *J. Cell Biol.* **163**, 1089-1098.
Ronen, D. and Ravid, S. (2009). Myosin II tailpiece determines its paracrystal structure, filament assembly properties, and cellular localization. *J. Biol. Chem.* **284**, 24948-24957.
Rosenberg, M. and Ravid, S. (2006). Protein kinase Cgamma regulates myosin IIB phosphorylation, cellular localization, and filament assembly. *Mol. Biol. Cell* **17**, 1364-1374.
Rosse, C., Linch, M., Kermorgant, S., Cameron, A. J., Boeckeler, K. and Parker, P. J. (2010). PKC and the control of localized signal dynamics. *Nat. Rev. Mol. Cell Biol.* **11**, 103-112.
Sheffield, P., Garrard, S. and Derewenda, Z. (1999). Overcoming expression and purification problems of RhoGDI using a family of 'parallel' expression vectors. *Protein Expr. Purif.* **15**, 34-39.
Shohet, R. V., Conti, M. A., Kawamoto, S., Preston, Y. A., Brill, D. A. and Adelstein, R. S. (1989). Cloning of the cDNA encoding the myosin heavy chain of a vertebrate cellular myosin. *Proc. Natl. Acad. Sci. USA* **86**, 7726-7730.
Simons, M., Wang, M., McBride, O. W., Kawamoto, S., Yamakawa, K., Gdula, D., Adelstein, R. S. and Weir, L. (1991). Human nonmuscle myosin heavy chains are encoded by two genes located on different chromosomes. *Circ. Res.* **69**, 530-539.
Sripathy, S., Lee, M. and Vasioukhin, V. (2011). Mammalian Llgl2 is necessary for proper branching morphogenesis during placental development. *Mol. Cell. Biol.* **31**, 2920-2933.
Strand, D., Jakobs, R., Merdes, G., Neumann, B., Kalmes, A., Heid, H. W., Husmann, I. and Mechler, B. M. (1994). The Drosophila lethal(2)giant larvae tumor suppressor protein forms homo-oligomers and is associated with nonmuscle myosin II heavy chain. *J. Cell Biol.* **127**, 1361-1373.
Straussman, R., Ben-Ya'acov, A., Woolfson, D. N. and Ravid, S. (2007). Kinking the coiled coil—negatively charged residues at the coiled-coil interface. *J. Mol. Biol.* **366**, 1232-1242.
Vasioukhin, V. (2006). Lethal giant puzzle of Lgl. *Dev. Neurosci.* **28**, 13-24.
Verkhovsky, A. B., Svitkina, T. M. and Borisy, G. G. (1999). Self-polarization and directional motility of cytoplasm. *Curr. Biol.* **9**, 11-20.
Vicente-Manzanares, M., Zareno, J., Whitmore, L., Choi, C. K. and Horwitz, A. F. (2007). Regulation of protrusion, adhesion dynamics, and polarity by myosins IIA and IIB in migrating cells. *J. Cell Biol.* **176**, 573-580.
Vicente-Manzanares, M., Koach, M. A., Whitmore, L., Lamers, M. L. and Horwitz, A. F. (2008). Segregation and activation of myosin IIB creates a rear in migrating cells. *J. Cell Biol.* **183**, 543-554.
Vicente-Manzanares, M., Ma, X., Adelstein, R. S. and Horwitz, A. R. (2009). Non-muscle myosin II takes centre stage in cell adhesion and migration. *Nat. Rev. Mol. Cell Biol.* **10**, 778-790.
Yamanaka, T., Horikoshi, Y., Sugiyama, Y., Ishiyama, C., Suzuki, A., Hirose, T., Iwamatsu, A., Shinohara, A. and Ohno, S. (2003). Mammalian Lgl forms a protein complex with PAR-6 and aPKC independently of PAR-3 to regulate epithelial cell polarity. *Curr. Biol.* **13**, 734-743.

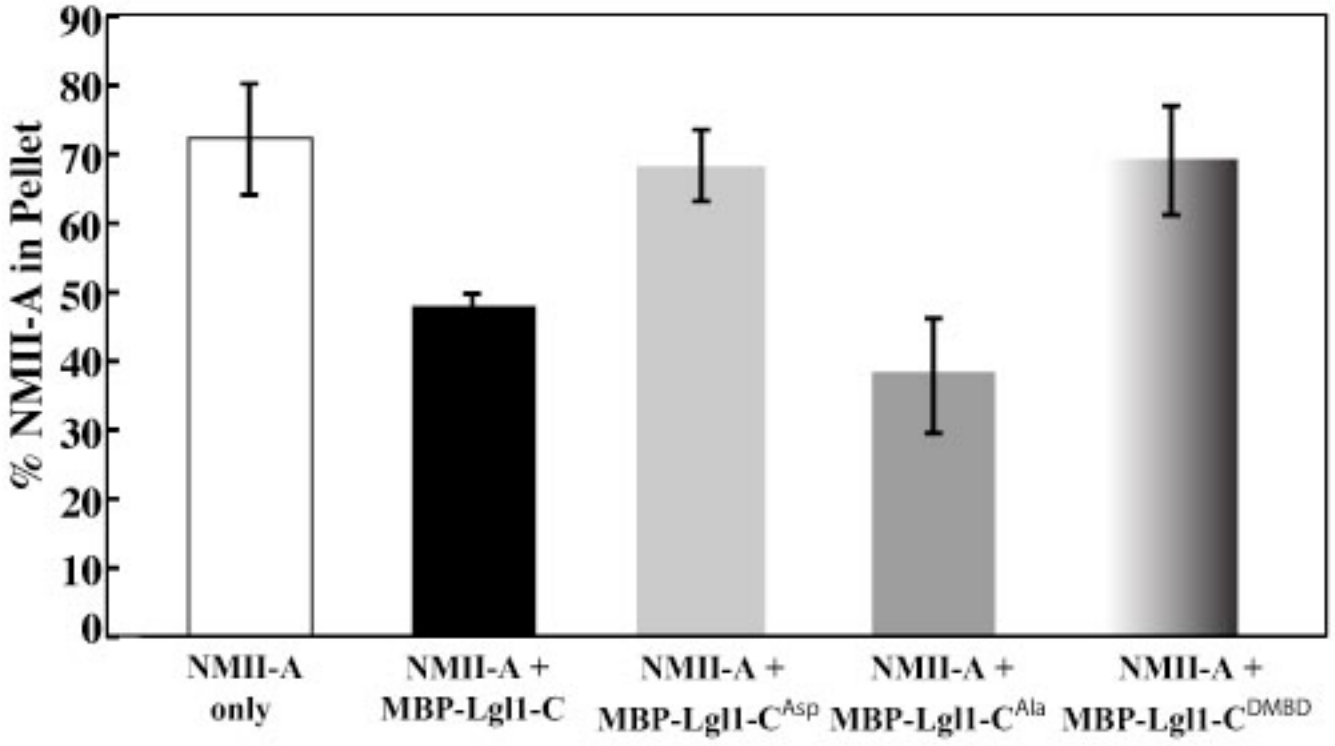

Fig. S1. Phosphorylation of Lgl1 affects NMII-A filament assembly. NMII-A Rods alone or with MBP-Lgl1 C-terminal protein fragments were subjected to a filament assembly assay. MBP-Lgl1-$C^{\Delta MBD}$ was used as a negative control. Assays were performed using a buffer containing 10 mM phosphate buffer, pH 7.5, 2 mM $MgCl_2$, and 150 mM NaCl. Values represent the mean ± SD for three independent experiments.

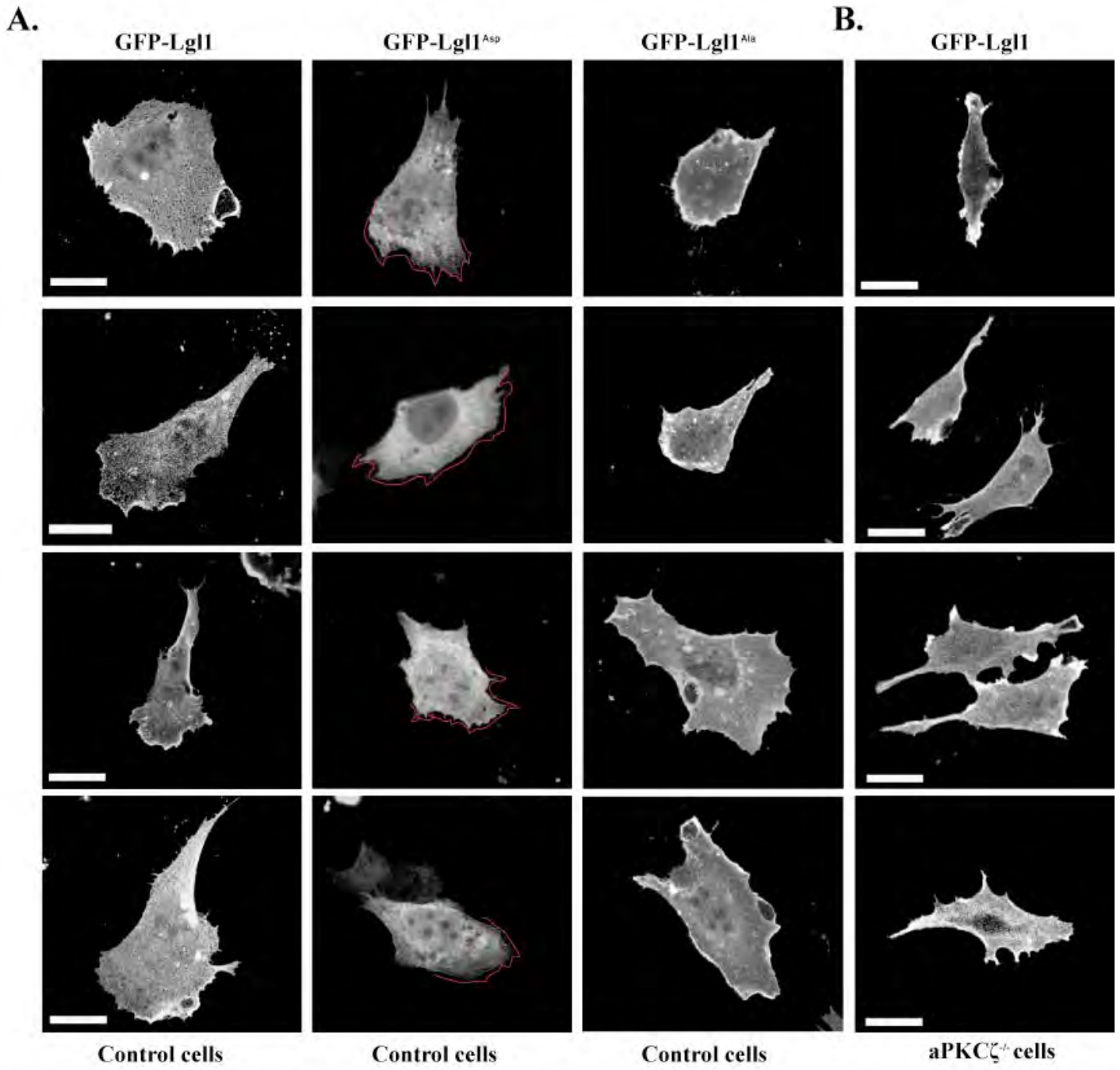

Fig. S2. Gallery of cells representing the effects of Lgl1 phosphorylation on its cellular localization. Control cells transfected with GFP-Lgl1, GFP-Lgl1^{Ala} or GFP-Lgl1^{Asp} (**A**) and aPKCζ$^{-/-}$ cells transfected with GFP-Lgl1 (**B**) were seeded on coverslips and subjected to a scratch wound assay. Red line in the GFP-Lgl1^{Asp} columns indicates the cell's leading edge as determined by F-actin staining. The cells were visualized using inverted confocal microscopy. Bars, 20 μm.

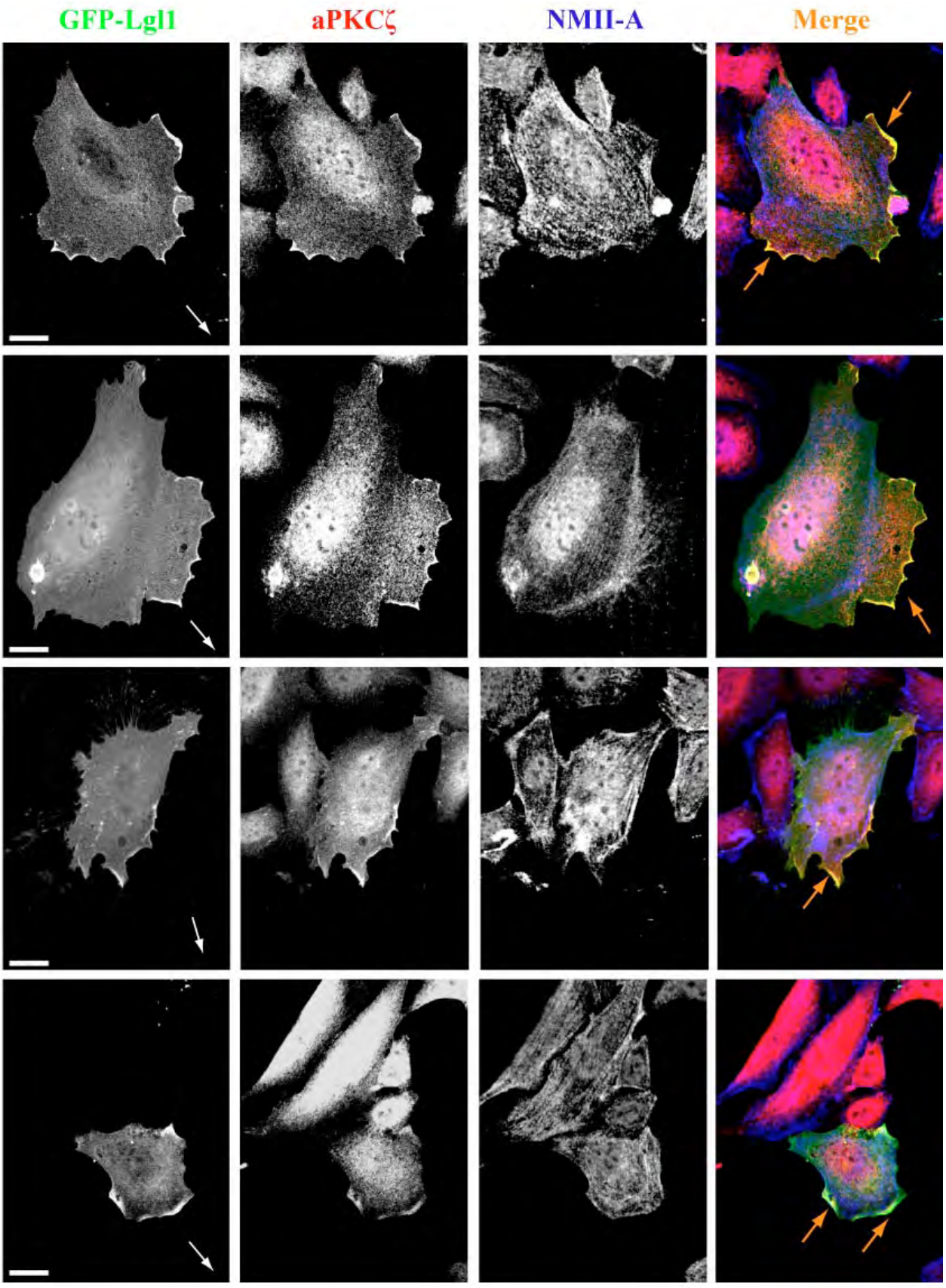

Fig. S3. Gallery of cells representing the colocalization of Lgl1 and aPKCζ at the cell leading edge. Control cells transfected with GFP-Lgl1 were seeded on coverslips and subjected to a scratch wound assay, stained for NMII-A using C-terminal-specific antibody conjugated to Cy5 and aPKCζ with specific antibody conjugated to rhodamine. White and orange arrows indicate the direction of cell migration and the co-localization of GFP-Lgl1 and aPKCζ, respectively. Bars, 20 μm.

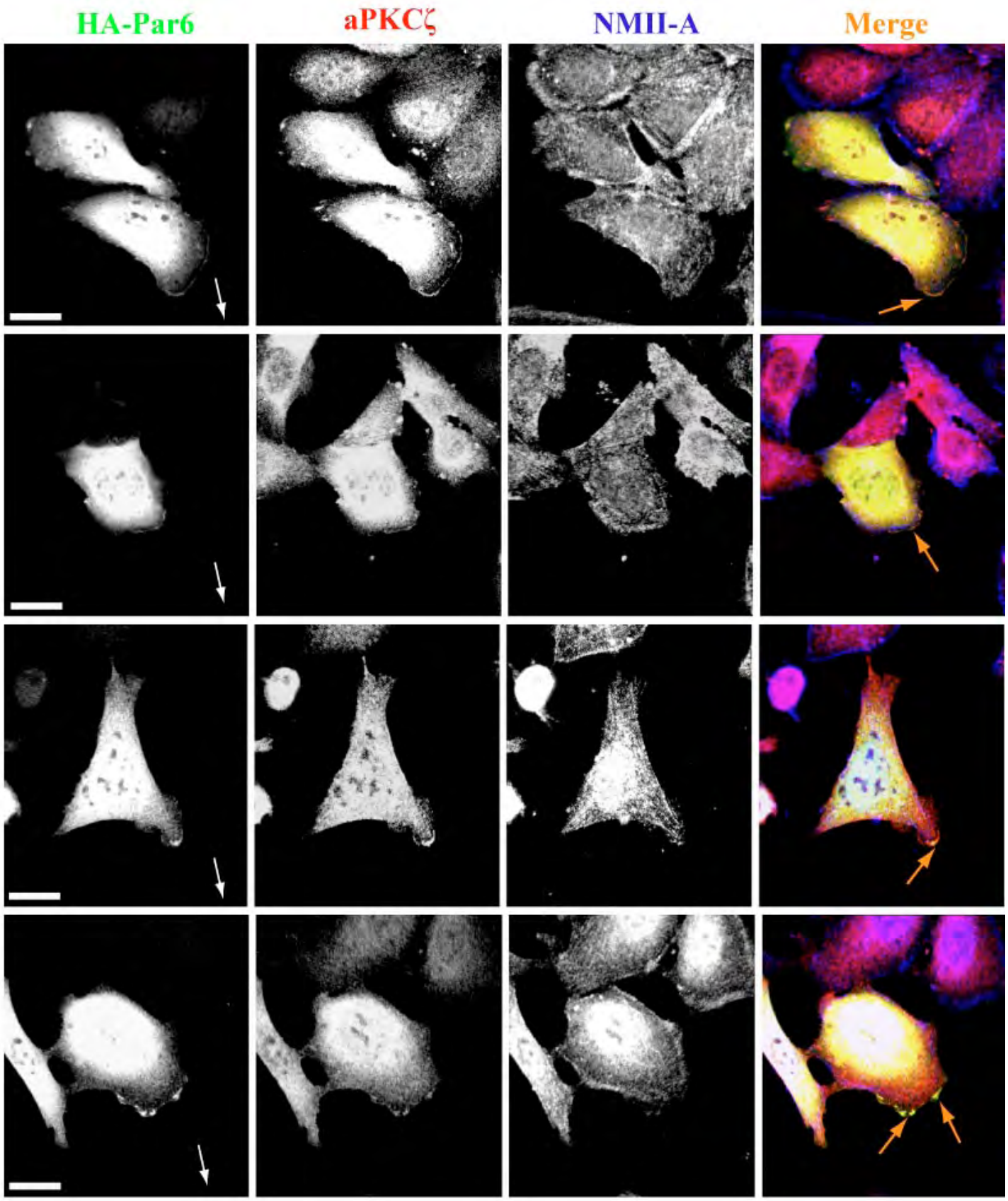

Fig. S4. Gallery of cells representing the colocalization of aPar6α and aPKCζ at the cell leading edge. Control cells transfected with HA-Par6α were seeded on coverslips and subjected to a scratch wound assay, stained for HA-Par6α using HA-specific antibody conjugated to FITC, NMII-A using C-terminal-specific antibody conjugated to Cy5 and aPKCζ with specific antibody conjugated to rhodamine. White and orange arrows indicate the direction of cell migration and the colocalization of HA-Par6α and aPKCζ, respectively. Bars, 20 μm.